AI-Driven Design of Microwave Antennas with Case Studies

Mobayode O. Akinsolu
Faculty of Arts, Science and Technology
Wrexham Glyndŵr University
Wrexham LL11 2AW, UK
mobayode.akinsolu@glyndwr.ac.uk

***Abstract*—With the advent of artificial intelligence (AI), the design of microwave devices such as antennas has been expedited in terms of throughput and time-to-market. This is chiefly because design automation via optimization has replaced the use of time intensive manual design techniques which premise on trial and error without any guarantee of successful outcomes. For the rapid design of antennas via optimization, surrogate model-based optimization (SMBO) methods tend to be at the forefront due to their efficiency improvement in terms of computational cost. The surrogate model assisted differential evolution for antenna synthesis (SADEA) algorithm family are a class of state-of-the-art SMBO methods. In this paper, the use and advantages of the SADEA algorithm family is demonstrated using two cases of real-world antenna design problems as examples. The antenna design problems are the optimization of: a multi-layered compact multiple-input and the multiple-output (MIMO) antenna array for wireless communications and a microwave imaging antenna for ultra wide band (UWB) body-centric applications. For both examples, the SADEA algorithm family obtained very good design solutions within an affordable time and the quality of the obtained solutions are validated by the close agreement which exits between the simulated and measured results of the fabricated and ready-to-use prototypes of the antennas. For both cases, the performance of the SADEA algorithm family is compared with 2019 Computer Simulation Technology - Microwave Studio (CST-MWS) optimizers (trust region framework (TRF) and particle swarm optimisation (PSO)). Results from the comparisons show that the SADEA algorithm family obtains very satisfactory design solutions in all runs using an affordable optimization time in each, whereas the alternative optimizers failed in all runs by not meeting the design requirements and/or generating designs with geometric incongruities.**

***Index Terms*—Antenna optimization; Artificial intelligence; Evolutionary methods; PSADEA; SADEA; SADEA-II; Surrogate model-based optimization.**

I. Introduction

Artificial intelligence (AI) continues to play a very significant role in microwave engineering. In the last few decades, the design and development of microwave devices such as antennas has been efficiently expedited using state-of-the-art machine learning and computational techniques which are built on AI paradigms [1]–[4]. Conventionally, microwave devices (antennas in particular) can be designed by following rules of thumb which are often validated using design experience [4], [5]. Whilst these rules adequately serve as practical guide for antenna designers and engineers, their judicious use and application often lead to sub-optimal antenna designs [4], [5]. This is typically the case when the design criteria and performance specifications are very stringent and highly reliant on the geometric profiles and/or material composition of the antennas [4]. Therefore, antenna designers and engineers are in the practice of tuning the parameters of sub-optimal antenna designs generated by manual techniques for better performance. This process is highly laborious and there is no guarantee of successful outcomes as it is often based on trial and error. To address the above challenges, antenna design automation via optimization must be carried out to generate near-optimal antenna designs and structures.

Local optimization and global optimization are the two fundamental ways of carrying out antenna optimization. For local optimization methods, a very good initial design, which is seldom available in practice, is required to obtain good or reasonably acceptable design solutions. Consequently, global optimization methods are more attractive due to their robustness and optimization capacity, not requiring an initial design. AI techniques such as evolutionary computation have chiefly informed the development of global optimization methods, in particular evolutionary algorithms (EAs). EAs such as differential evolution (DE) [6] and particle swarm optimisation (PSO) [7] tend to be at the forefront of widely used global optimization methods for antenna synthesis. However, global optimization methods such as EAs often require a large number a large number of full-wave electromagnetic (EM) simulations to obtain good or reasonably acceptable design solutions [8].

For antennas to be accurately characterized for performance estimation and evaluation, numerical technique-based EM simulations (e.g., time domain analysis using the finite integration technique (FIT)) which are computationally expensive are required [5], [9]. As a result, the optimization time becomes excessively long (or even prohibitive in some cases) when EAs are used to synthesize antennas [4]. To address the challenge of long optimization time, efficiency improvement methods which can adequately lower the overall computation cost of the optimization without much compromise on the quality of the design solutions generated by the optimization procedure are required. Surrogate model-based optimization (SMBO) is a very promising optimization efficiency improvement method. AI techniques including machine learning and statistical modelling are the primary features of SMBO.

By means of machine learning and statistical modelling,

SMBO methods build and employ surrogate models which are cheap approximation models of the exact evaluations to replace computationally expensive exact function evaluations (e.g., EM simulations). Surrogate model-assisted evolutionary algorithms (SAEAs) are built when EAs are used as the search engine in SMBO methods [10], [11]. There exists a vital trade-off between the quality of the surrogate model and the efficiency (premised on the essential number of exact evaluations) in SAEAs. Thus, a surrogate model management method is required to find an appropriate trade-off in SAEAs. Due to a multiplicity of surrogate model management procedures, there are various kinds of SAEAs. The surrogate model-aware evolutionary search (SMAS) framework is a state-of-the-art SAEA framework and its efficiency and optimization quality are well established and verified [10]–[13].

The surrogate model assisted differential evolution for antenna synthesis (SADEA) algorithm family are a class of SMAS-based SAEAs purpose-built for antenna design synthesis [14]–[16]. They offer 3 to 20 times speed improvement compared to global optimization methods and they have been widely applied to several challenging real-world design problems. The main recurring features across all the SADEA generations in the SADEA algorithm family are DE global search and Gaussian process (GP) surrogate modelling. The first generation SADEA [14], [17], [18], called SADEA-I in this paper is suitable for antenna design problems of around 10 up to 30 dimensions, while the second generation SADEA [17], called SADEA-II in this paper is suitable for the efficient synthesis of computationally expensive multi-fidelity antennas with the same dimensionality limit as SADEA-I.

The state-of-the-art in the SADEA algorithm is the third generation SADEA, parallel surrogate model assisted hybrid differential evolution for antenna optimisation [16], [19], called SADEA-III in this paper. SADEA-III is developed for use in parallel computing environments where multiple candidate designs can be simulated concurrently using distributed processors and shared memory on multicore operating systems. SADEA-III employs multiple DE mutation strategies and reinforcement learning techniques to achieve an added 1.5 to 3 times efficiency improvement and higher design solution quality even in the sequential mode compared to the previous generations of SADEA [16], [19].

The primary goal of this paper is to demonstrate the use and advantages of the SADEA algorithm family as an industry-standard for the efficient AI-driven design of microwave antennas using real-world antenna design problem case studies as examples. All examples considered are finished and ready-to-use industry standard antenna products and the optimization capacity of the SADEA algorithm family is compared to widely used and commercially available antenna optimizers. The remainder of the paper is organized as follows: Section II provides the generic framework of the SADEA algorithm family and highlights the distinctions across all the generations. Section III presents the performance of the SADEA algorithm family using two real-world industry standard antennas and comparisons between the performance of the SADEA algorithm family and 2019 CST-MWS optimizers are made. The concluding remarks are given in Section IV.

II. SADEA Algorithm Family Framework

As mentioned above, the key elements in the framework of the SADEA algorithm family across all generations are Gaussian process (GP) surrogate modelling and differential evolution (DE) global search [16], [19]. Given a set of observations, GP predicts the function value at a design point by modelling the function as a Gaussian distributed stochastic variable with a known mean and variance. The mean squared error (MSE) of the prediction uncertainty is then deduced and the lower confidence bound method is used to evaluate the quality of a candidate design with respect to the predicted value. More details on how GP machine learning is adopted across all generations can be found in [14], [14], [16], [19]. The DE search engine in all SADEA generations follows the standard convention of generating child solutions for donor vectors via mutation and crossover operations in the optimization process. More details on how the DE algorithm works can be found in [6].

Generically, the SADEA algorithm family adopt the following basic steps in their modus operandi:

- **Step 1:** Sample a small number of designs from the design space using the Latin Hypercube sampling (LHS) method [20] and perform EM simulations on these designs to build the initial database.
- **Step 2:** If a preset stopping condition (e.g. the maximum number of EM simulations) is met, output the best design from the database; otherwise go to Step 3.
- **Step 3:** Select a number of best designs from the database to create a population.
- **Step 4:** Apply DE operators on the population in Step 3 to produce child populations and their respective child solutions.
- **Step 5:** For each candidate design in each population, build a GP (Gaussian process) model using training data points created from the nearest designs based on Euclidean distance from the database and their performance values.
- **Step 6:** Use the GP (Gaussian process) models in Step 5 and the lower confidence bound (LCB) prescreening method [21] to prescreen the child solution(s) generated in Step 4. Select the top-ranked child solution(s) according to the LCB values.
- **Step 7:** Evaluate the estimated top-ranked child solution(s) from Step 6 by simulating them. Add them and their performances (via simulation) to the database. Go back to Step 2.

The main distinctions across the generations of the SADEA algorithm family are summarized as follows: (1) In SADEA-I, only the DE/best/1 mutation operator is applied at Step 4 and in steps 6 and 7 only one child solution is considered [14], [17], [18]. (2) In SADEA-II, a three-stage optimization involving Steps 1 to 7 (as in SADEA-I) using a coarse model at the first stage, data mining at the second stage and steps 1 to 7 (as in SADEA-I, but enhanced by a local search using the best design from stage 1 as the starting point) using fine model at the last stage is carried out [15]. (3) In SADEA-III, a self-adaptive DE/best/1, DE/current-to-best/1 and DE/rand/2-

based search is involved at Step 4 and as a result three child solutions are considered in steps 6 and 7 [16], [19]. SADEA-III is the direct augmentation of SADEA-I because both follow the same procedural routines and both can be applied to similar antenna design problems.

III. Case Studies

Using two real-world antennas, the use and advantages of the SADEA algorithm family are demonstrated in this section. The example antennas for the case studies are a multi-layered compact MIMO antenna array for wireless applications and a microwave imaging antenna for UWB body-centric applications. More case studies (including the optimization of: a base station antenna for 5G applications, a highly compact crossed-dipole antenna for global navigation satellite system (GNSS) applications and a dual-band circularly polarized elliptical patch antenna for global positioning system (GPS) and Iridium applications) showing the optimization capacity of the SADEA algorithm family are available at: https://ai-dac.com/antenna-design-gallery/. The time consumption reported in the case studies is wall clock time.

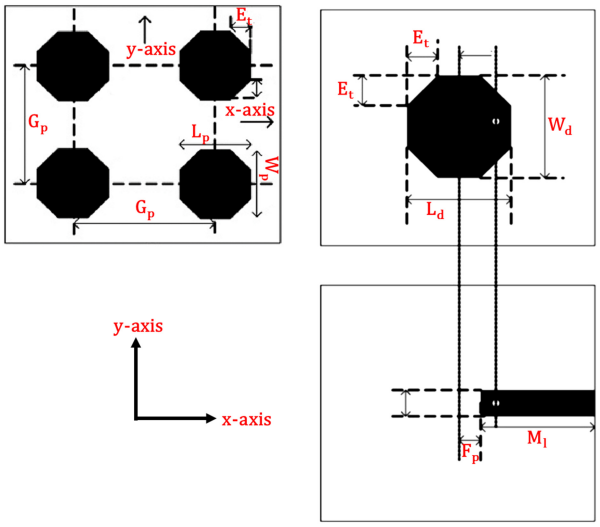

Figure 1. A cross section of the layout of the multilayered compact MIMO antenna array (example 1).

A. Example 1: Multilayered Compact MIMO (Multiple-Input and Multiple-Output) Antenna Array

The first example is the 8-variable two-port (reconfigurable) compact MIMO antenna array for wireless applications [22]. It is implemented on a stacked multi-layered structure which mainly consists of six dielectric substrate layers, a ground plane, eight parasitic patches and a driven radiator. The antenna configuration borrows some ideas from [23] and a cross section of its layout is shown in Fig. 1. Four of the antenna's parasitic patches are implemented on the first substrate, the driven radiator is implemented on the second substrate, the ground plane is interposed between the third and fourth substrates, the second feed line is implemented on the fifth substrate and the remaining four parasitic patches are implemented on the sixth dielectric substrate.

Table I
Search ranges of the design variables and the optimal design by SADEA-I (all sizes in mm) (Example 1)

N^o	$Variables$	Lower bound	Upper bound	SADEA-I Optimum
1	Length of the driven patch (L_d)	12	18	17.39
2	Uniform length of the parasitic patches (L_p)	10	20	16.44
3	Width of the driven patch (W_d)	12	18	14.55
4	Uniform width of the parasitic patches (W_p)	10	20	15.60
5	Uniform gap between the four parasitic patches (G_p)	12	40	19.19
6	Microstrip line length (M_l)	-9	9	-8.70
7	Relative position of feed coupling (F_p)	0.25	30	3.02
8	Uniform edge tapering of all patches (E_t)	0.5	10	3.93
9	$(L_p + 2 - G_p) \leq 0$			
10	$\{G_p - 2\times \min([30-\frac{L_p}{2}\text{ -5, 30 - }\frac{W_p}{2} - 5])\} \leq 0$			
11	$\{-\frac{L_d}{2} + \text{abs}(M_l)\} \leq 0$			
12	$\{E_t - min(\left[\frac{L_d}{2}, \frac{W_d}{2}, \frac{L_p}{2}, \frac{W_p}{2}\right])\} \leq 0$			

The first, third, fourth and sixth substrate layers are made of RO4003C laminate which has a thickness of 3.048 mm, relative permittivity (ϵ_r) of 3.38 and a dielectric loss tangent (tan(δ)) of 0.0027, while the second and fifth substrate layers are made of RT/duroid 6006 laminate which has a thickness of 1.9 mm thick, relative permittivity (ϵ_r) of 6.17 and dielectric loss tangent (tan(δ)) of 0.0025. The two feeding ports are terminated using 50Ω microstrip lines and they are orthogonal (note that this is not shown in the cross section in Fig. 1, but it is revealed later on in Fig. 2(a)). The parasitic patches are electromagnetically coupled to the driven elements. The compact MIMO antenna array is modelled and discretized in CST-MWS using the time domain FIT method with an accuracy of -30 dB and a maximum cell density of 10 cells per wavelength resulting in about 200,000 hexahedral mesh cells in total. Each simulation costs about 1.5 minutes on a workstation with Intel 4-core i7 CPU and 24GB RAM.

$$\text{minimize} \quad max|S_{11}| \quad 4.5GHz - 8.5GHz \qquad (1)$$

For the AI-driven synthesis of the compact MIMO antenna array, the design parameters, their given search ranges and the geometric constraints in Table I are considered. The optimization goal is the minimization of the maximum return loss over the operational bandwidth of 4.5 GHz to 8.5 GHz as shown in (1).

SADEA-I generates a design which obtains a max(S_{11}) of -10.3 dB in the bandwidth of interest after about 430 simulations in around 14 hours. Note that CST-MWS antenna optimizers were employed to synthesize this antenna without any recorded success after several runs requiring hundreds of EM simulations. A typical result using 2019 CST-MWS TRF

obtains a max(S_{11}) of -3 dB in the bandwidth of interest after several hundreds of EM simulations. The physical implementation of the SADEA-I synthesized design as a finished and ready-to-use product is shown in Fig. 2(a). The simulation and measurement results for the free space return loss are shown in Fig. 2(b) and it can be observed that they are in close agreement.

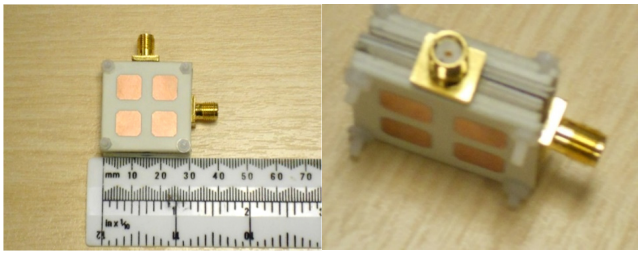

(a) Physical implementation of SADEA-I synthesized design.

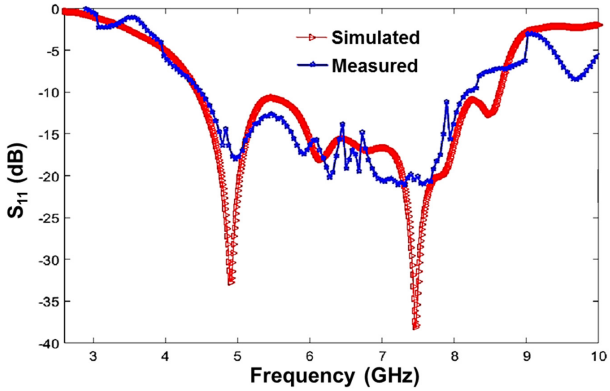

(b) Free space return loss.

Figure 2. The multilayered compact MIMO antenna array (example 1).

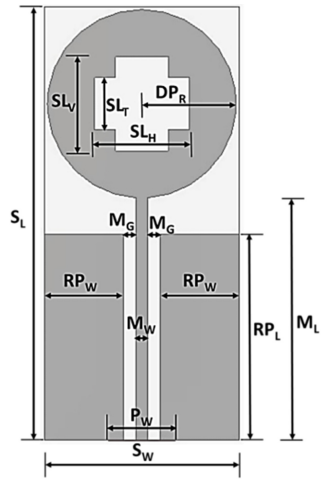

(a) Layout of the primitive design.

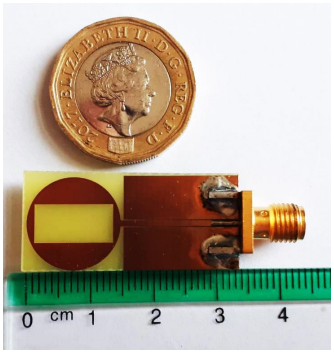

(b) Physical implementation of SADEA-III synthesized design.

Figure 3. The microwave imaging antenna (example 2).

B. Example 2: Microwave Imaging Antenna

The second example is the 10-variable microwave imaging antenna for UWB body-centric applications [24]. The layout of its primitive design is as shown in Fig. 3(a). It primarily consists of two uniform rectangular planes which form a co-planar partial ground, a circular radiator fed by a 50Ω microstrip line with four T slots which are fused at the head centrally etched on it. The microwave imaging antenna is implemented on an FR-4 substrate having a loss tangent (tan(δ)) of 0.025, a relative permittivity (ϵ_r) of 4.3 and a thickness of 0.8 mm. It is modelled and discretized in CST-MWS using the time domain analysis FIT method with an accuracy of -40 dB with a maximum cell density of 20 cells per wavelength resulting in about 300,000 hexahedral mesh cells in total. Each simulation costs about 2 minutes on the average on a workstation with Intel 4-core i7 CPU and 24GB RAM.

For the AI-driven synthesis of the microwave imaging antenna, the design parameters, their given search ranges and the geometric constraints in Table II are considered. The optimization goal is the minimization of the fitness function (F_{mon}) in (2) to achieve the design specifications in Table III. For the comparisons, the computing budget are as follows: 500 parallel simulations (i.e., 1500 EM simulations in total considering three simulations are carried out in parallel [16], [19]) over 10 runs for SADEA-III, 3000 simulations over five runs and 5000 simulations over three runs are used for 2019 CST-MWS TRF and 2019 CST-MWS PSO, respectively. Additional runs are not affordable for 2019 CST-MWS PSO and 2019 CST-MWS TRF because a single run costs several days. Note that for 2019 CST-MWS TRF, all initial designs for each run are randomly generated using the LHS (Latin Hypercube sampling) method [20] and sigma is set to unity to direct search towards a global optimum.

$$F_{mon} = max(S_{11}) + w \times max([2\,dBi - G_{min}, 0]) + ... \\ w \times max([G_{max} - 5\,dBi, 0]) \tag{2}$$

where w is the penalty coefficient and it is set to 50. The set value for w preferentially ensures that the specifications for the bore-sight gain in Table III (i.e., G_{min} and G_{max}) are satisfied first by largely penalizing F_m if they are violated. Then, meeting the S_{11} requirement becomes the main focus of the optimization procedure as soon as the G_{min} and G_{max} requirements are satisfied.

After 2.5 days of optimization, SADEA-III obtains the design shown in Table II and the performance for this design is shown in Table III. The physical implementation of the

Table II
SEARCH RANGES OF THE DESIGN VARIABLES AND A TYPICAL OPTIMAL DESIGN BY SADEA-III (ALL SIZES IN MM) (EXAMPLE 1)

N^o	$Variables$	Lower bound	Upper bound	SADEA-III Optimum
1	Substrate width (S_W)	$2 \times DP_R$	$3 \times DP_R$	14.90
2	Microstrip length (M_L)	20.00	50.00	18.52
3	Microstrip width (M_W)	0.50	7.50	0.84
4	Microstrip gap (M_G)	>0.00	21.50	0.12
5	Circular patch radius (DP_R)	2.00	25.00	7.21
6	Width of slot throat (SL_T)	>0.00	$2 \times DP_R$	5.98
7	Vertical slots' depth (SL_V)	>0.00	$2 \times DP_R$	12.06
8	Horizontal slots' depth (SL_H)	>0.00	$2 \times DP_R$	5.98
9	Partial ground plane length (RP_L)	DP_R	M_L	18.05
10	Feed guide width (P_W)	$6 \times M_W$	$10 \times M_W$	2.56
11	Substrate length (S_L) = M_L+(2 $\times$ DP_R)+ 0.2 mm			
12	Partial ground plane width (RP_w) = (S_W-(2 $\times$ M_G)-M_W) $\div$ 2			

Table III
PERFORMANCE SPECIFICATIONS FOR EXAMPLE 1: UWB (3.1 GHz TO 10.6 GHz)

N^o	Item	Specifications	SADEA-III Optimum
1	Maximum return loss (S_{11})	$\leq$ -10 dB	-10.6 dB
2	Minimum bore-sight gain (G_{min})	$\geq$ 2 dBi	2.2 dBi
3	Maximum bore-sight gain (G_{max})	$\leq$ 5 dBi	4.7 dBi

SADEA-III synthesized design as a finished and ready-to-use product is shown in Fig. 3(b) and the overall size is 33.14 mm $\times$ 14.90 mm $\times$ 0.8 mm, which is compact and about half the size (linear dimensions) of a similar-state-of-the-art design [25]. The simulated and measured results for the free space return loss and on-phantom return loss of the SADEA-III synthesized design are shown in Fig. 4(a) and Fig. 4(b), respectively. From Fig. 4(a) and Fig. 4(b), it can be seen that the simulated and measured results are in reasonable agreement. Also from Fig. 4(b), it can be seen that the microwave imaging antenna maintains its UWB operation and is not overly detuned in the presence of a human phantom modelled according to [26], [27].

The bore-sight gain requirements is met by all methods

Table IV
STATISTICS OF THE BEST MAX.(S_{11}) VALUES USING DIFFERENT METHODS (EXAMPLE 1)

$Method$	$Best$	$Worst$	$Mean$	$Median$	$Std.$
SADEA-III (10 runs)	-10.6 dB	-10.05 dB	-10.38 dB	-10.39 dB	0.1815
2019 CST-MWS TRF (5 runs)	N/A	N/A	N/A	N/A	N/A
2019 CST-MWS PSO (3 runs)	-5.92 dB	-5.02	-5.61	-5.90	0.5113

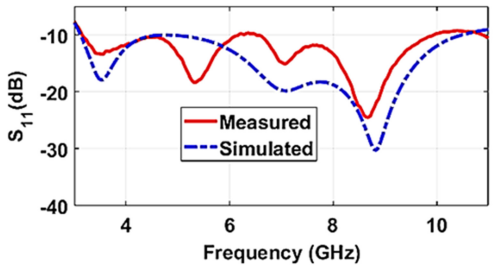

(a) Free space.

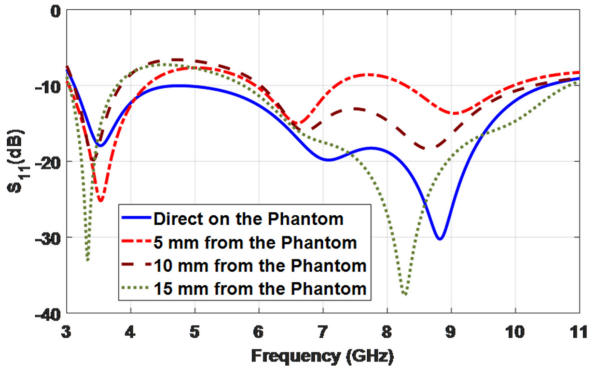

(b) On-phantom

Figure 4. Simulated and measured return loss for the SADEA-III optimized design of the monopole antenna.

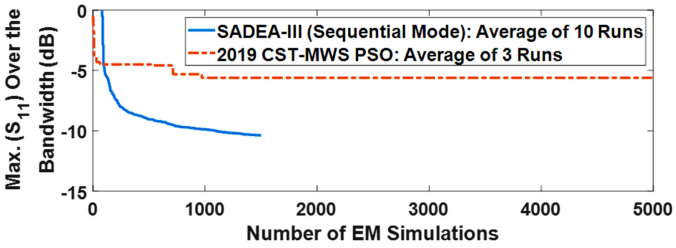

Figure 5. Convergence trends of SADEA-III and 2019 CST-MWS PSO (example 2).

over all runs. In terms of the quality of results, the following observations are made from Table IV for the return loss: (1) SADEA-III satisfies the return loss requirement in Table III in all 10 runs showing a very good result even for the worst case (2) A low standard deviation value for SADEA-III shows that it has good robustness. (3) 2019 CST-MWS TRF fails to satisfy the return loss requirement in Table III and generated designs with geometric incongruities in all five runs. Thus, 2019 CST-MWS TRF results are considered as not applicable (N/A). The rationale for this is that designs with geometric incongruities are impractical and cannot be fabricated for real-world use. (4) CST-MWS PSO fails to meet the return loss requirement in Table III in all three runs.

In terms of efficiency, the convergence trend is shown in Fig. 5. From Fig. 5, PSADEA uses an average of 1090 EM simulations to satisfy all the specifications in Table III and then converges to obtain an average max(S_{11}) of -10.38 dB after 1450 EM simulations. Also from Fig. 5, it can be observed that 2019 CST-MWS PSO obtains an average max(S_{11}) of -5.61 dB after 972 EM simulations with no significant improvement

over 5000 EM simulations. To obtain the result of 2019 CST-MWS PSO, PSADEA needs 127 EM simulations on average. Hence, it can be deduced that PSADEA is 7.7 times faster than 2019 CST-MWS PSO on the average for this example. Note that the convergence trend for 2019 CST-MWS TRF is not shown in Fig. 5 because it is N/A due to geometric incongruities as earlier mentioned.

IV. Conclusions

In this paper, the optimization capacity of the SADEA algorithm family is demonstrated using two real-world antenna design problems as case studies. For the first antenna design problem, which is the optimization of a multi-layered compact MIMO antenna array for wireless communications, a very good design solution ready for fabrication was obtained by SADEA-I in less than a day. For the second antenna design problem, which is the optimization of a microwave imaging antenna for UWB body-centric applications, SADEA-III obtained a very good design solution ready for fabrication in less than three days. For both problems, the efficiency of the SADEA algorithm family is revealed. 2019 CST-MWS optimizers were applied to both problems without any successful outcome after several runs using hundreds of EM simulations. The quality of the design solutions obtained by the SADEA algorithm family is validated through the physical implementation of the optimal design for the MIMO antenna array and a typical optimal design for the microwave imaging antenna. A close agreement is found to exist between the measured and simulated results for the fabricated prototypes.

References

[1] J. Moreno, I. González, and D. Rodríguez, "Design of a TTC antenna using simulation and multiobjective evolutionary algorithms," *IEEE Aerospace and Electronic Systems Magazine*, vol. 34, no. 7, pp. 18–31, 2019.

[2] L. Wang, X. Zhang, and X. Zhang, "Antenna array design by artificial bee colony algorithm with similarity induced search method," *IEEE Transactions on Magnetics*, vol. 55, no. 6, pp. 1–4, 2019.

[3] N. H. Shrifan, M. F. Akbar, and N. A. M. Isa, "Prospect of using artificial intelligence for microwave nondestructive testing technique: A review," *IEEE Access*, vol. 7, pp. 110 628–110 650, 2019.

[4] V. Grout, M. O. Akinsolu, B. Liu, P. I. Lazaridis, K. K. Mistry, and Z. D. Zaharis, "Software solutions for antenna design exploration: A comparison of packages, tools, techniques, and algorithms for various design challenges," *IEEE Antennas and Propagation Magazine*, vol. 61, no. 3, pp. 48–59, 2019.

[5] T. Weiland, M. Timm, and I. Munteanu, "A practical guide to 3-D simulation," *IEEE Microwave Magazine*, vol. 9, no. 6, pp. 62–75, 2008.

[6] R. Storn and K. Price, "Differential evolution–a simple and efficient heuristic for global optimization over continuous spaces," *Journal of global optimization*, vol. 11, no. 4, pp. 341–359, 1997.

[7] J. Kennedy, "Particle swarm optimization," *Encyclopedia of machine learning*, pp. 760–766, 2010.

[8] M. Mognaschi, "Micro biogeography-inspired multi-objective optimisation for industrial electromagnetic design," *Electronics Letters*, vol. 53, no. 22, pp. 1458–1460, 2017.

[9] K. K. Mistry, P. I. Lazaridis, Z. D. Zaharis, M. O. Akinsolu, B. Liu, T. D. Xenos, I. A. Glover, and R. Prasad, "Time and frequency domain simulation, measurement and optimization of log-periodic antennas," *Wireless Personal Communications*, pp. 1–13, 2019.

[10] B. Liu, H. Yang, and M. J. Lancaster, "Global optimization of microwave filters based on a surrogate model-assisted evolutionary algorithm," *IEEE Transactions on Microwave Theory and Techniques*, vol. 65, no. 6, pp. 1976–1985, 2017.

[11] B. Liu, V. Grout, and A. Nikolaeva, "Efficient global optimization of actuator based on a surrogate model assisted hybrid algorithm," *IEEE Transactions on Industrial Electronics*, vol. 65, no. 7, pp. 5712–5721, 2017.

[12] B. Liu, Q. Zhang, and G. G. Gielen, "A gaussian process surrogate model assisted evolutionary algorithm for medium scale expensive optimization problems," *IEEE Transactions on Evolutionary Computation*, vol. 18, no. 2, pp. 180–192, 2013.

[13] B. Liu, Q. Chen, Q. Zhang, G. Gielen, and V. Grout, "Behavioral study of the surrogate model-aware evolutionary search framework," in *2014 IEEE Congress on Evolutionary Computation (CEC)*. IEEE, 2014, pp. 715–722.

[14] B. Liu, H. Aliakbarian, Z. Ma, G. A. Vandenbosch, G. Gielen, and P. Excell, "An efficient method for antenna design optimization based on evolutionary computation and machine learning techniques," *IEEE Transactions on Antennas and Propagation*, vol. 62, no. 1, pp. 7–18, 2013.

[15] B. Liu, S. Koziel, and N. Ali, "SADEA-II: A generalized method for efficient global optimization of antenna design," *Journal of Computational Design and Engineering*, vol. 4, no. 2, pp. 86–97, 2017.

[16] B. Liu, M. O. Akinsolu, N. Ali, and R. Abd-Alhameed, "Efficient global optimisation of microwave antennas based on a parallel surrogate model-assisted evolutionary algorithm," *IET Microwaves, Antennas & Propagation*, vol. 13, no. 2, pp. 149–155, 2018.

[17] B. Liu, A. Irvine, M. O. Akinsolu, O. Arabi, V. Grout, and N. Ali, "GUI design exploration software for microwave antennas," *Journal of Computational Design and Engineering*, vol. 4, no. 4, pp. 274–281, 2017.

[18] M. O. Akinsolu, F. M. Abdussalam, O. Arabi, B. Liu, R. A. Abd-Alhameed, N. Ali, G. Ibrahim, and T. Rashid, "Antenna design explorer: A GUI software tool for efficient antenna design optimization," in *2017 Loughborough Antennas and Propagation Conference (LAPC)*. Loughborough, UK, 2017, pp. 1–5.

[19] M. O. Akinsolu, B. Liu, V. Grout, P. I. Lazaridis, M. E. Mognaschi, and P. Di Barba, "A parallel surrogate model assisted evolutionary algorithm for electromagnetic design optimization," *IEEE Transactions on Emerging Topics in Computational Intelligence*, vol. 3, no. 2, pp. 93–105, 2019.

[20] M. Stein, "Large sample properties of simulations using latin hypercube sampling," *Technometrics*, pp. 143–151, 1987.

[21] M. T. Emmerich, K. C. Giannakoglou, and B. Naujoks, "Single-and multiobjective evolutionary optimization assisted by gaussian random field metamodels," *IEEE Transactions on Evolutionary Computation*, vol. 10, no. 4, pp. 421–439, 2006.

[22] O. Arabi, N. Ali, B. Liu, R. Abd-Alhameed, and P. Excell, "Compact MIMO antenna array design for wireless applications," in *Antenna Fundamentals for Legacy Mobile Applications and Beyond*. Springer, 2018, pp. 173–190.

[23] Z. Chen *et al.*, "Multipatches multilayered uwb microstrip antennas," *IET microwaves, antennas & propagation*, vol. 3, no. 3, pp. 379–386, 2009.

[24] I. M. Danjuma, M. O. Akinsolu, B. Muhammad, E. Eya, R. Abd-Alhameed, J. M. Noras, and B. Liu, "A compact size and low profile rectangular slot monopole antenna for UWB body centric applications," in *2019 IEEE International Symposium on Antennas and Propagation and USNC-URSI Radio Science Meeting*. Georgia, USA, Accepted Paper: In-press.

[25] B. Yeboah-Akowuah, P. Kosmas, and Y. Chen, "A q-slot monopole for UWB body-centric wireless communications," *IEEE Transactions on Antennas and Propagation*, vol. 65, no. 10, pp. 5069–5075, 2017.

[26] B. B. Beard, W. Kainz, T. Onishi, T. Iyama, S. Watanabe, O. Fujiwara, J. Wang, G. Bit-Babik, A. Faraone, J. Wiart *et al.*, "Comparisons of computed mobile phone induced sar in the sam phantom to that in anatomically correct models of the human head," *IEEE transactions on electromagnetic compatibility*, vol. 48, no. 2, pp. 397–407, 2006.

[27] C.-H. Lin, K. Saito, M. Takahashi, and K. Ito, "A compact planar inverted-F antenna for 2.45 ghz on-body communications," *IEEE Transactions on Antennas and Propagation*, vol. 60, no. 9, pp. 4422–4426, 2012.